Magnetotransport properties of flux melt grown single crystals of Co-substituted manganites with perovskite structure

2003 J. Phys.: Condens. Matter 15 925

(http://iopscience.iop.org/0953-8984/15/6/319)

INSTITUTE OF PHYSICS PUBLISHING JOURNAL OF PHYSICS: CONDENSED MATTER

J. Phys.: Condens. Matter **15** (2003) 925–936 PII: S0953-8984(03)38468-1

Magnetotransport properties of flux melt grown single crystals of Co-substituted manganites with perovskite structure

D D Khalyavin[1,5], M Pekala[2], G L Bychkov[1], S V Shiryaev[1], S N Barilo[1], I O Troyanchuk[1], J Mucha[3], H Misiorek[3], R Szymczak[4], M Baran[4] and H Szymczak[4]

[1] Institute of Solid State and Semiconductors Physics, National Academy of Sciences, P. Brovka Street 17, 220072 Minsk, Belarus
[2] Department of Chemistry, University of Warsaw, Al. Zwirki i Wigury 101, PL-02-089 Warsaw 22, Poland
[3] Institute of Low Temperature and Structure Research, Polish Academy of Sciences, ulica Okólna 2, 50-422 Wroclaw, Poland
[4] Institute of Physics, Polish Academy of Sciences, Al. Lotnikow 32/46, PL 02-668 Warsaw, Poland

E-mail: khalyav@ifttp.bas-net.by

Received 21 June 2002, in final form 18 September 2002
Published 3 February 2003
Online at stacks.iop.org/JPhysCM/15/925

Abstract

Single crystals of $La_{1-x}Ba_xMn_{1-y}Co_yO_3$ ($0.26 \leqslant x \leqslant 0.37$; $0 \leqslant y \leqslant 0.31$) perovskites were grown by the flux melt technique using the $BaO–B_2O_3–BaF_2$ ternary system as a solvent. It was found that the cobalt content in the crystals is determined by the average oxidized state of the manganese ions and depends nonlinearly on the molar ratio of Co/Mn in the initial mixture. All the crystals exhibit ferromagnetic behaviour at low temperatures as well as a jump of resistivity and a magnetoresistance peak around the Curie temperature, gradually decreasing as the cobalt content increases. The low-temperature ferromagnetic phase transforms from the metallic to the semiconducting state with increase in cobalt content.

1. Introduction

The effect of Mn-site doping by different transition metals on the properties of manganites ($Ln_{1-x}A^{2+}_xMn_{1-y}Me_yO_3$ Ln—lanthanide, A^{2+}—alkaline-earth metals, Me—transition metal) has been reported by many researchers [1–5]. However, these investigations have mostly been done on polycrystalline samples, which complicates the interpretation of the obtained

[5] Author to whom any correspondence should be addressed.

results, especially with regard to transport properties. On the other hand, preparation of high-quality single crystals is a difficult task requiring much care. Of the different 3d elements that may be introduced instead of manganese, cobalt ions are remarkable since the Mn^{4+}–O–Co^{2+} superexchange interaction is strongly ferromagnetic [6]. The charge state of cobalt ions incorporated into manganese-based perovskite oxides has been a matter of discussion in many papers [6–12]. Recent complex spectroscopic investigations [9, 11, 12] unambiguously indicate the $Co^{2+} + Mn^{4+}$ ionic configuration to be more stable than the $Co^{3+} + Mn^{3+}$ one. This fact is very important, and has to be taken into account in the analysis of the exchange interactions and electrical properties of Co-substituted manganites. In the present work we report growing conditions for Co-substituted manganites with the flux melt technique using the $BaO–B_2O_3–BaF_2$ ternary system as the solvent as well as some magnetic and electrical properties of the obtained crystals. Recently the aforementioned method was successfully applied to obtain large ($\sim$1 cm^3) high-quality single crystals of Ba-substituted manganites [13]. In particular, it is established that the concentration of Ba^{2+} ions in the $La_{1-x}Ba_xMnO_3$ single crystals can be changed within the interval ($0.2 < x < 0.5$) by varying the growth temperature (T_g), whereas the ratio of the solvent component does not influence this parameter so significantly. So in this work we used a ternary solvent with a fixed molar ratio of the components, $52.39BaO–19.29BaF_2–28.32B_2O_3$, and changed only the content and component ratio of the crystal oxides formed.

2. Crystal growth

$La_{1-x}Ba_xMn_{1-y}Co_yO_3$ single crystals were grown by the flux melt technique in the dynamic regime using the $52.39BaO–19.29BaF_2–28.32B_2O_3$ ternary system as the solvent. Growth was carried out in a vertical furnace provided with SiC heaters. The home-modified RIF-101 temperature controller allowed the temperature to be stabilized with an accuracy of $\pm 0.1\,^{\circ}$C and provided the capability to scan the temperature at a rate as low as $0.1\,^{\circ}$C/day. The cation ratios of La:Ba and Mn:Co in the crystals were determined by x-ray fluorescent analysis. The chemical composition was written starting from data normalized to 1. The perturbation of the main elements was realized by using either a ^{241}Am ($\gamma = 59.54$ keV) or a ^{109}Cd ($\gamma = 22.16$; 88.0 keV) radioisotope source. The x-ray spectrometer with an Si(Li)-semiconductor detector was used to register the secondary characteristic radiation from a ^{55}Fe radioisotope source with an accuracy of 200 eV at the 5.95 keV line. The flux melt was prepared by successive melting of 99.99% purity initial components separately weighed in the corresponding ratios. Lanthanum oxide was annealed for 24 h at $1200\,^{\circ}$C before weighing to avoid flux creep due to considerable wetting of the platinum crucible. Having determined the saturation (T_{sat}) and spontaneous crystallization temperatures, three or four separate crystals were allowed to grow up to a size of 6–10 mm^3 at a constant temperature which was 1–2 $^{\circ}$C lower than T_{sat}. The fluctuations in chemical composition for crystals obtained in the same growth cycle did not exceed $\Delta x = \pm 0.02$ and $\Delta y = \pm 0.03$. Some experimental details are presented in table 1.

The cobalt content in the $La_{1-x}Ba_xMn_{1-y}Co_yO_3$ crystals with an average Ba concentration $x \sim 0.36 \pm 0.02$ as a function of Co/Mn molar ratio in the initial mixture used for the flux melt preparation is shown in figure 1. It is obvious that the distribution coefficient of cobalt $k = C_{cr}/C_{fm}$ (where C_{cr} is the Co/Mn molar ratio in the crystals and C_{fm} is the same ratio in the flux melt) is very low ($k \ll 1$). Moreover, a stoichiometric coefficient y of Co in the general chemical formula of the crystals rises nonlinearly with increase of the Co/Mn molar ratio in the initial mixture. The highest value of $y = 0.31$ in the crystals with barium content $x \sim 0.36 \pm 0.02$ was reached at a molar ratio of 5.45. A further increase in Co content in the

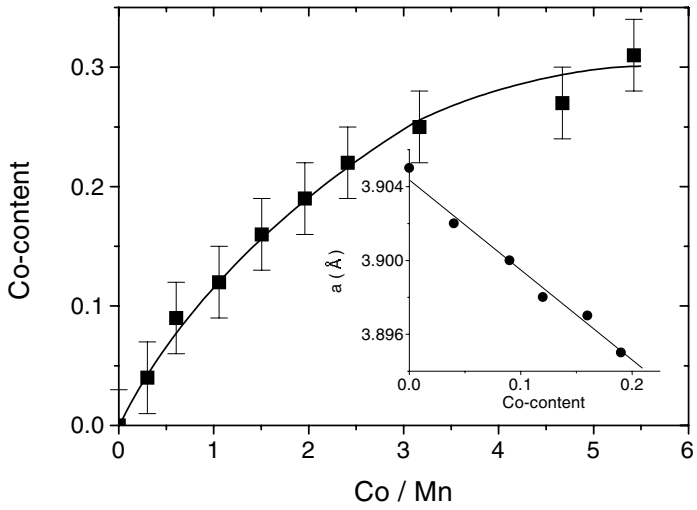

Figure 1. Cobalt content in $La_{1-x}Ba_xMn_{1-y}Co_yO_3$ ($x \sim 0.36 \pm 0.02$) crystals as a function of the Co/Mn molar ratio in the initial mixture. Inset: parameter of a pseudo-cubic unit cell versus Co content in the crystals.

Table 1. Selected data on flux growth of $La_{1-x}Ba_xMn_{1-y}Co_yO_3$ single crystals using $52.39BaO–19.29BaF_2–28.32B_2O_3$ as the solvent.

Sample number	Total content of solute in flux (wt%)	Co/Mn molar ratio in flux	Growth temperature (°C)	Co content in crystals, y	Ba content in crystals, x
1	9.55	—	989	—	0.37
2	10.09	0.30	996	0.04	0.37
3	10.66	0.61	996	0.09	0.37
4	11.51	1.05	997	0.12	0.37
5	12.33	1.51	996	0.16	0.37
6	13.09	1.96	1009	0.19	0.38
7	13.86	3.16	1039	0.25	0.33
8	17.52	4.66	1013	0.27	0.34
9	18.72	5.45	1013	0.31	0.33
10	23.45	3.75	1173	0.27	0.25

initial mixture leads to an inconsistent increase in the viscosity of the flux melt which prevents steady growth and co-crystallization of the CoO phase with the doped manganite phase. Phase transformations and crystal structure distortions were determined by x-ray diffraction study. According to the data, crystals of the $La_{1-x}Ba_xMn_{1-y}Co_yO_3$ series with $x > 0.3$ are characterized by a pseudo-cubic crystal structure in the whole concentration range of cobalt ($0 < y < 0.31$). The unit cell volume decreases monotonically as the Co content increases (figure 1, inset). In contrast, the structure of the crystals with a lower barium concentration ($x < 0.3$) has considerable rhombohedral distortions at room temperature.

3. Measurements

Magnetization measurements were performed using a commercial SQUID magnetometer (Quantum Design MPMS-5) in a magnetic field up to 50 kOe. Electrical resistivity was

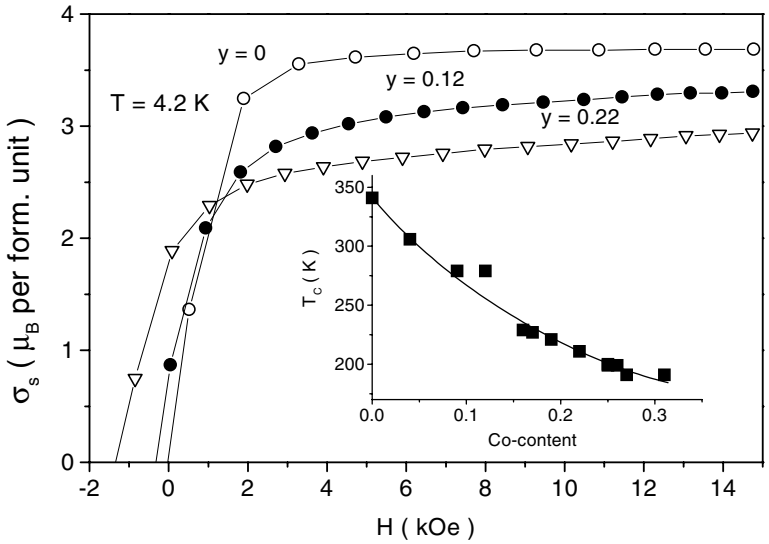

Figure 2. Part of the hysteresis loop showing the magnetization of $La_{1-x}Ba_xMn_{1-y}Co_yO_3$ ($x \sim 0.36 \pm 0.02$) single crystals as a function of magnetic field recorded after cooling at $H = 16$ kOe. Inset: dependence of the Curie temperature on the cobalt content of the crystals.

measured by a conventional dc four-probe method with a temperature stabilization accuracy of 0.01 K. Thermoelectric power and thermal conductivity were measured using an absolute method with a temperature gradient of 0.2 K created along the sample. The time of temperature stabilization between two consecutive experimental points varied from 15 min at temperatures of the order of 10 K to about 1 h above 78 K. Particular care was taken to avoid parasitic heat transfer between the sample and the environment. The sample was placed inside a cylindrical screen made of material displaying a thermal conductivity similar to that of the sample. Temperature variation along the screen identical to the temperature gradient along the sample was set up. The mean temperature of the sample and the screen also coincided. Both current and voltage leads were thermally anchored to the screen. The measurement error was $\pm 2\%$ and the surplus error, estimated from the scatter in the measurement points, did not exceed $\pm 0.2\%$. The experimental set-up and the procedure has been described in detail in [14].

4. Results

4.1. Magnetic properties

According to magnetization measurements all the $La_{1-x}Ba_xMn_{1-y}Co_yO_3$ crystals obtained are ferromagnetic at low temperature with values of spontaneous magnetization (σ_S) and Curie temperature that gradually decrease with an increase in cobalt content (figure 2, inset). For example, the σ_S for $La_{0.63}Ba_{0.37}Mn_{0.78}Co_{0.22}O_3$ amounted to $\sim 2.5\ \mu_B$ per formula unit. This value of σ_S is relatively lower than that in the case of fully ferromagnetic ordering of both cobalt and manganese ions. Apparently the magnetic moments of cobalt ions are randomly oriented relative to the magnetic moments of manganese, depending on their local surroundings. Magnetization behaviour at weak fields strongly depends on barium content in the crystals, as shown in figure 3. Pseudo-cubic crystals with a relatively high Ba content do not exhibit any anomaly below the magnetic ordering temperature, whereas rhombohedral samples with a

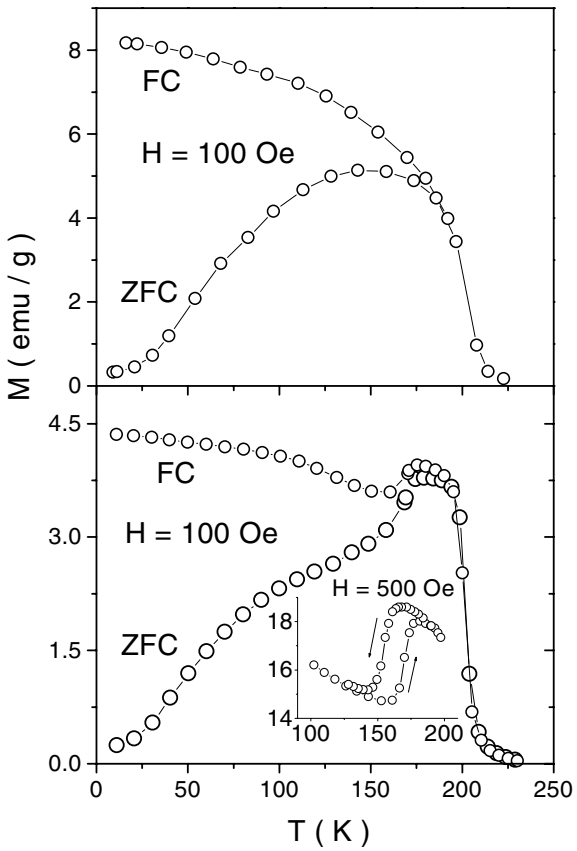

Figure 3. Field cooled (FC) and zero-field cooled (ZFC) magnetization as a function of temperature for $La_{0.63}Ba_{0.37}Mn_{0.78}Co_{0.22}O_3$ (upper panel) and $La_{0.72}Ba_{0.28}Mn_{0.78}Co_{0.22}O_3$ (bottom panel) single crystals. Inset: temperature hysteresis of magnetization around the point (T_t) of the low-temperature phase transition.

comparatively low Ba content show a sharp enhancement of magnetization near $T_t = 160$ K. This anomaly is accompanied by a large temperature hysteresis (figure 3, inset) associated with the first-order phase transition. This abnormal behaviour is suppressed by a magnetic field and disappears at $H > 5$ kOe. A similar behaviour of the magnetization has been observed in Co-free $La_{0.8}Ba_{0.2}MnO_3$ single crystals grown by the floating zone technique and was attributed to the change of magnetic anisotropy caused by transformation of the crystal structure from the orthorhombic ($Pbnm$) to the rhombohedral ($R\bar{3}c$) phase with increase in temperature [15]. The temperature dependence of magnetization for $La_{0.74}Ba_{0.26}Mn_{0.86}Co_{0.14}O_3$ crystals registered at H parallel to [100], [010] and [001] directions has revealed a considerable anisotropy for both orthorhombic and rhombohedral phases (figure 4). Since in the rhombohedral phase all these orientations seem to be equivalent, the observed magnetic anisotropy for this phase in low magnetic fields is probably caused by partial conservation of the domain structure attributed to the orthorhombic phase.

4.2. Magnetoresistance

Temperature dependences of resistivity for $La_{1-x}Ba_xMn_{1-y}Co_yO_3$ ($x \sim 0.28 \pm 0.02$) single crystals with different cobalt contents $y = 0.12$, 0.16 and 0.22 are shown in figure 5. A

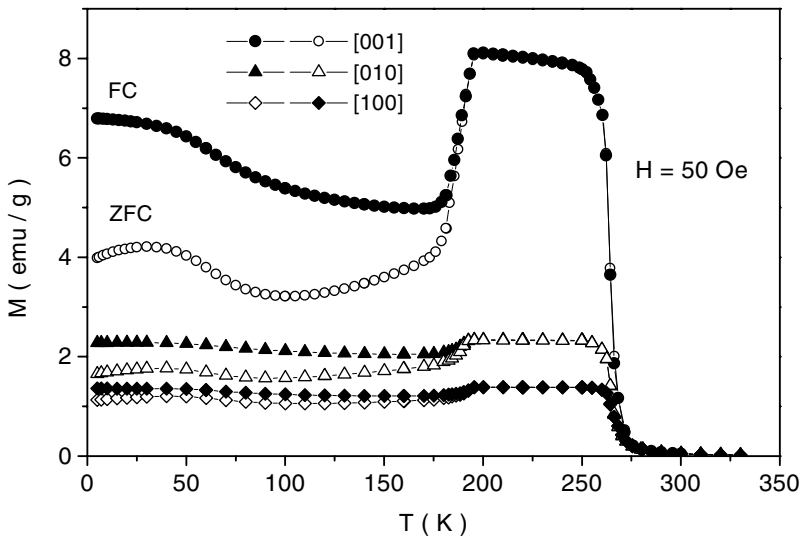

Figure 4. Temperature dependence of magnetization for $La_{0.74}Ba_{0.26}Mn_{0.86}Co_{0.14}O_3$ registered along different orientations of the crystal. The crystallographic directions are determined for the low-temperature orthorhombic phase.

pronounced maximum of resistivity, which is a characteristic of interplay between magnetism and electrical transport, was found for all the crystals at temperatures close to T_C. However, the resistivity behaviour of the crystals with $y = 0.12$ and 0.22 at low temperatures is quite different (see figure 5). One can see that the low-temperature phase is metallic for the crystal with $y = 0.12$ whereas reentrant transition into the insulating phase takes place in the crystal with $y = 0.22$. The resistivity value for the metallic crystal $La_{0.74}Ba_{0.26}Mn_{0.86}Co_{0.14}O_3$ is of the order of 40 $\mu\Omega$ at 200 K (figure 6, upper panel), confirming the high quality of the single crystal, and is comparable to that for thin films of $La_{2/3}Ba_{1/3}MnO_x$ [16]. Figure 6 also shows that no distinct change of resistivity is observed around the transition from the low-temperature orthorhombic phase to the high-temperature rhombohedral one at 180 K. As shown in figure 6, the measured resistance is strongly affected by magnetic field strength. The height of the resistivity maximum is gradually suppressed with increasing magnetic field up to 80 kOe, accompanied by its broadening at higher magnetic fields. It is shown in the inset of figure 6 that the position of the electrical resistance maximum for $La_{0.74}Ba_{0.26}Mn_{0.86}Co_{0.14}O_3$ crystal shifts towards higher temperatures with increasing magnetic field. Isofields of MR (MR $= [(R(H = 0) - R(H))/R(H = 0)]$) temperature variation are plotted in the bottom panel of figure 6. A sharp maximum of negative magnetoresistance occurs at a temperature slightly below that of the resistivity peak. Almost all the crystals exhibit a similar magnitude of magnetoresistance despite different behaviour of the electrical resistivity (figure 4, bottom panel).

4.3. Thermoelectric power

Measurements of the dependence of thermoelectric power on temperature, $S(T)$ were also undertaken for metallic $La_{0.74}Ba_{0.26}Mn_{0.86}Co_{0.14}O_3$ crystals (figure 7). The values of S are positive and relatively low (about 11 μV K^{-1}), both at room temperature and 40 K. A pronounced minimum down to 1 μV K^{-1} was observed at 100 K. No remarkable changes

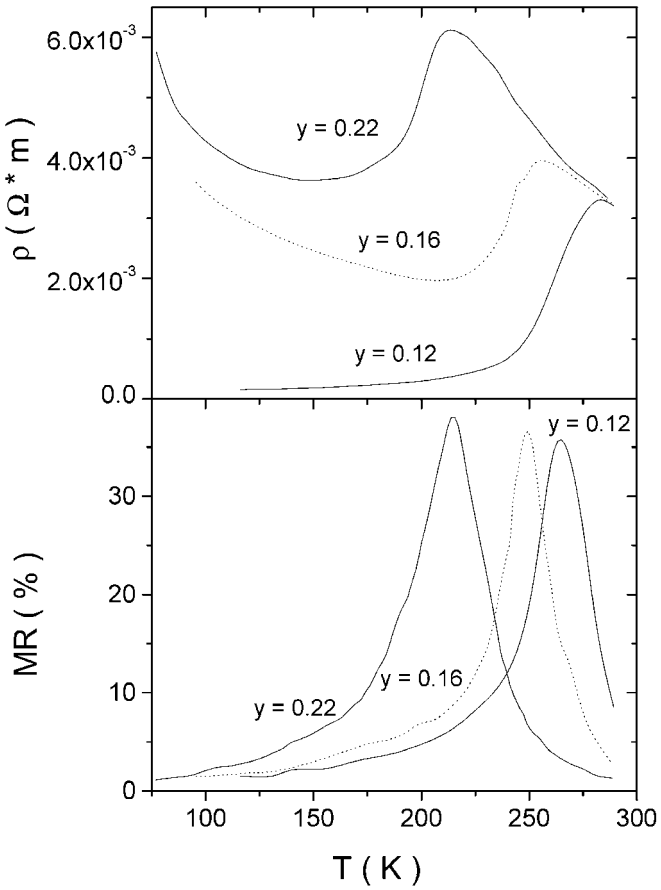

Figure 5. Temperature dependences of resistivity (upper panel) and magnetoresistance at applied field $H = 10$ kOe (bottom panel) for a set of $La_{1-x}Ba_xMn_{1-y}Co_yO_3$ ($x \sim 0.28 \pm 0.02$) single crystals with different cobalt contents y.

in thermoelectric power were found at temperature around 180 K, corresponding to the aforementioned transition in the crystal structure. An additional kink appears on the $S(T)$ curve at the temperature $T = 265$ K where transition into the paramagnetic state takes place.

4.4. Thermal conductivity

The thermal conductivity, k, of the $La_{0.74}Ba_{0.26}Mn_{0.86}Co_{0.14}O_3$ crystal varies smoothly from 0.05 W m^{-1} K^{-1} at helium temperature to 0.55 W m^{-1} K^{-1} at 300 K (figure 8). Such low values of thermal conductivity are typically observed in solids with a strongly disordered structure [17]. But a disordered solid approach is not applicable for the single crystals studied here. The registered temperature variation of thermal conductivity is qualitatively similar to the k behaviour of non-metallic manganites ($La_{1-x}A_xMnO_3$A = Ca, Sr) in the low-doped range $x < 0.15$ as reported by Cohn *et al* [18] and Visser *et al* [19], who suggested distortions caused by large anharmonicity to be the origin of the magnitude of reduction of thermal conductivity. Conversely an appreciable enhancement of thermal conductivity has been reported for optimally doped manganites $x \sim 0.3$ at the temperature of transition into

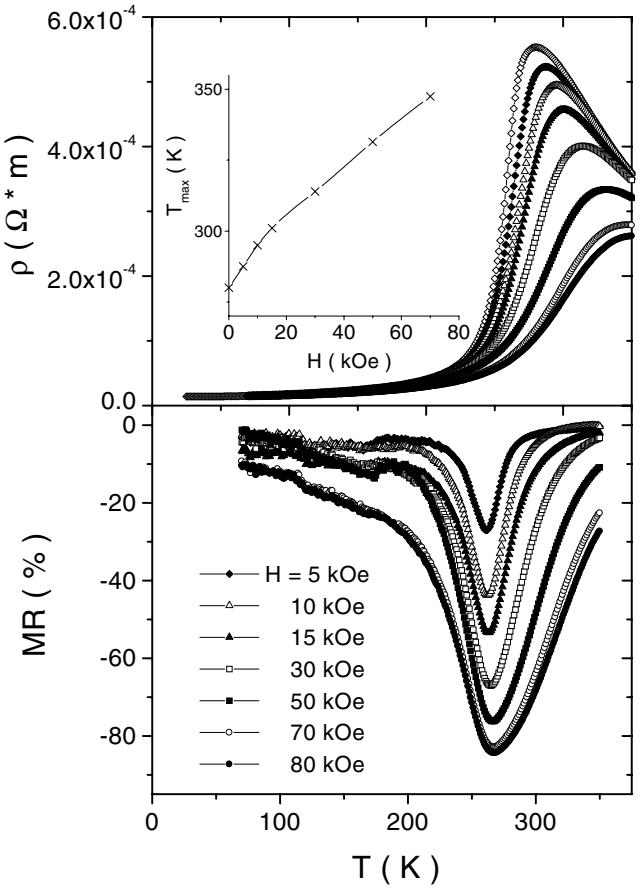

Figure 6. Temperature dependences of resistively (upper panel) and magnetoresistance (bottom panel) for $La_{0.74}Ba_{0.26}Mn_{0.86}Co_{0.14}O_3$ crystal registered at different magnetic fields. Inset to upper panel: the temperature of the resistivity maximum in dependence on applied magnetic field.

the ferromagnetic metallic state. The Wiedemann–Franz law

$$k_e(T) = L_0 T/\rho(T) \tag{1}$$

where $L_0 = 2.45 \times 10^{-8}$ W Ω K^{-2} is the Lorentz number, allows one to estimate a reasonable upper limit for the electronic contribution to thermal conductivity in the free electron approximation. Using the Wiedemann–Franz law and resistivity data Salamon and Jaime found that the electronic contribution k_e to the thermal conductivity of $La_{0.67}(CaPb)_{0.33}MnO_3$ and $La_{0.2}Nd_{0.4}Pb_{0.4}MnO_3$ single crystals in the low-temperature metallic phase is no larger than 20% of their total thermal conductivity $k = k_e + k_{ph}$ (k_{ph} being the phonon contribution) [20]. Therefore the appearance of the metallic state in the optimally doped manganites can be used to explain only qualitatively the low-temperature increase in k. Taking into account these results, the following conclusion has been made [20]. Because of the nature of the very small magnetoelastic polarons, which appear in the paramagnetic phase as temperature is reduced, and the delocalization of charge carriers, the effective rate of electron–phonon scattering decreases and both the components of thermal conductivity, k_e and k_{ph}, increase in the metallic state. We have not observed any anomalies on the $k(T)$ curve for $La_{0.74}Ba_{0.26}Mn_{0.86}Co_{0.14}O_3$

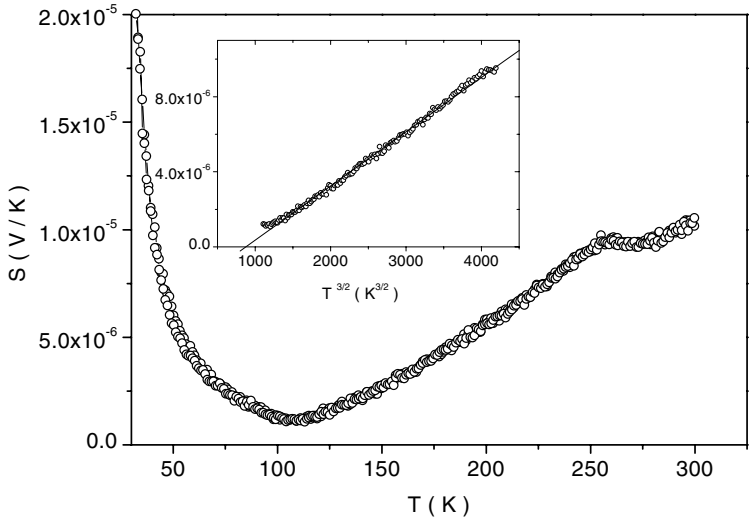

Figure 7. Thermoelectric power as a function of temperature for the $La_{0.74}Ba_{0.26}Mn_{0.86}Co_{0.14}O_3$ crystal. Inset: a fitting to the magnon drag contribution (in accordance with expression (2)).

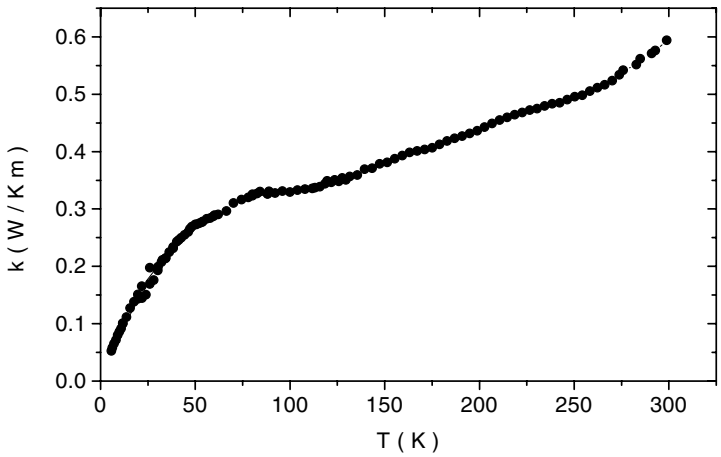

Figure 8. Thermal conductivity of $La_{0.74}Ba_{0.26}Mn_{0.86}Co_{0.14}O_3$ crystal in dependence on temperature.

crystal around $T_C \sim 265$ K where a distinct transition into the metallic state occurs. Thermal conductivity rises roughly in proportion to temperature in the range between 4 and 50 K, where processes of phonon scattering on impurities and crystal structure defects dominate. The crossover appears between 50 and 100 K, and k again increases linearly with temperature above 100 K. According to electrical resistivity data for $La_{0.74}Ba_{0.26}Mn_{0.86}Co_{0.14}O_3$ crystal (figure 6) a relatively large electronic contribution, $\sim$30%, to k should be expected at low temperatures $T < T_C$ in the case of a homogeneous metallic state. However, in fact a linear temperature dependence of the $k(T)$ dependence in the range $100 < T < 290$ K, without a noticeable anomaly at T_C, points to the absence of an appreciable electronic contribution in the low-temperature metallic phase and allows one to presume invariance of phonon scattering mechanisms both below and above T_C.

5. Discussion

According to x-ray absorption and XPS measurements of the $La_{0.7}Sr_{0.3}(Mn_{0.8}Co_{0.2})O_3$ [10] and $Pr_{0.5}Ca_{0.5}Mn_{0.95}Co_{0.05}O_3$ [12] perovskites the dopant Co takes the divalent state in these compounds. The NMR data also provide evidence for Co^{2+} and Mn^{4+} valence states in the ferromagnetic $La(Mn_{0.5}Co_{0.5})O_3$ [11]. Apparently the $Co^{2+} + Mn^{4+}$ ionic configuration is more stable than $Co^{3+} + Mn^{3+}$ for perovskites. The ferromagnetic behaviour of the $La_{1-x}Ba_xMn_{1-y}Co_yO_3$ single crystals with high cobalt content ($y > 0.15$) backs up this assumption since the superexchange interaction Mn^{4+}–O–Co^{2+} is always positive according to Goobenough–Kanamory rules. In contrast a small substitution (∼15%) of manganese ions by other divalent ions (Zn^{2+}, Mg^{2+}) leads to suppression of the ferromagnetic order [21]. On the other hand increase of Co^{2+} content results in a sharp enhancement of the average oxidized state of manganese ions and might be written as follows: $La_{1-x}Ba_x(Mn^{3+}_{1-x-2y}Mn^{4+}_{x+y}Co^{2+}_y)O_3$. We believe this fact is a dominant cause of the observed low distribution coefficient of cobalt under the flux growth process (figure 1). Apparently in the crystals grown under the above described conditions the maximum possible Co content is $y_{max} = (1 - x)/2$ when all manganese ions become tetravalent ($La_{1-x}Ba_xMn^{4+}_{(1+x)/2}Co^{2+}_{(1-x)/2}O_3$). Further increase in cobalt concentration in the flux melt leads to primary crystallization of the $Co^{2+}O$ phase. Therefore in order to grow crystals containing Co^{3+} ions either by the flux melt technique using $BaO–B_2O_3–BaF_2$ as the solvent or by other high-temperature growth methods one should provide a controlled environment near the crystallization front under optimal growth conditions (e.g. by varying the partial oxygen pressure inside the growth chamber).

The metallic behaviour of substituted rare earth manganites at low temperatures is suggested to be caused by a bond mechanism of conductivity. Electronic transfer in these compounds occurs due to the bond formed by hybridization between the e_g orbital of manganese and the 2p orbitals of oxygen [22, 23]. The value of the exchange interaction between spins of itinerant charge carriers and t_{2g}-localized electrons is comparable with the effective bandwidth, i.e. charge carriers can move only to the site with the same direction of spin providing hypothetical 100% spin polarization of the charge carriers at zero temperature. On the other hand such spin polarization may be the main reason for the dominant electron–magnon scattering leading to the T^2 dependence of resistivity versus temperature which has been found in these compounds [24]. The temperature variation of thermoelectric power in the doped manganites is strongly related to ferromagnetic ordering of manganese and may be described within the magnon drag model [25]. In the ferromagnetic region thermoelectric power S follows the expression

$$S = S_0 + S_{3/2}T^{3/2}. \tag{2}$$

Our thermoelectric power data for the $La_{0.74}Ba_{0.26}Mn_{0.86}Co_{0.14}O_3$ crystal fit well to expression (2) in a broad temperature region $100 < T < 260$ K, giving the values of $S_0 = -2.535\ \mu V\ K^{-1}$ and $S_{3/2} = 0.0029\ \mu V\ K^{-3/2}$ (figure 5, inset). The $T^{3/2}$ temperature dependence of S unambiguously confirms the contribution of a magnon drag to the thermoelectric power in this case. A phonon drag contribution, which could also be considered here, should vary with temperature as T^3 [26]. A large magnon drag effect was also observed in antiferromagnetic MnTe at high temperatures up to 310 K [27]. However, below 100 K one can see that the thermoelectric power begins to increase as temperature decreases whereas the crystal shows metallic conduction. Such behaviour may also be attributed to the development of insulating clusters within the metallic matrix. Apparently such crystal clusters are found at the metal–insulator concentration boundary where the localization process has a global character at the same time as the metallic phase percolation survives down to low temperatures. From

this viewpoint one can understand the low value of the electronic contribution to thermal conductivity k which was found in our case as well as the strong electron–phonon scattering below T_C. An additional increase in cobalt content in the crystal shifts the equilibrium and the low-temperature metallic phase transforms into a semiconductor. According to measurements of metallic $Pr_{0.5}Ca_{0.5}Mn_{0.95}Co_{0.05}O_3$ perovskite using soft x-ray absorption spectroscopy, Co^{2+} ions are characterized by a small charge transfer from the Co 3d band to the oxygen 2p band [12] which allows us to suggest that these Co ions do not participate directly in the conductivity phenomena. Hence the substitution of manganese with cobalt leads to decrease of the effective 3d bandwidth since Co^{2+}-substituted sites are not available to charge carriers. Moreover, Co^{2+} ions together with neighbouring Ba^{2+} ions can localize the Mn^{4+} holes due to electrostatic interactions contributing to the development of insulator clusters at low temperatures.

6. Conclusions

We investigated the growth conditions of Co-substituted lanthanum barium manganites grown by the flux melt technique using a $BaO–B_2O_3–BaF_2$ ternary system as the solvent. The cobalt content in the crystals is determined by the average oxidized state of the manganese ions and depends nonlinearly on the molar ratio of Co/Mn in the initial mixture. All the crystals exhibit ferromagnetic behaviour in spite of a concentration transition from the metallic into the semiconducting state as the Co content increases. The growth features and physical properties of the obtained crystals can be understood on the basis of the assumption that cobalt ions adopt only a divalent state.

Acknowledgments

The work was supported in part by Polish State Committee for Scientific Researches (Grants: 7T08A 02820, 5 P03B 016 20) and by Swiss National Scientific Foundation in frame of SCOPES program (Grant No 7 BYPJ 65732)

References

[1] Raveau B, Maignan A and Martin C 1997 *J. Solid State Chem.* **130** 162
[2] Bamabe A, Maignan A, Hervieu M, Damay F, Martin C and Raveau B 1997 *Appl. Phys. Lett.* **71** 3907
[3] Sun J R, Rao G H, Shen B G and Wong H K 1998 *Appl. Phys. Lett.* **73** 2998
[4] Li X-G X, Fan J, Ji G, Wu W B, Wong K H, Choy C L and Ku H C 1999 *J. Appl. Phys.* **85** 1663
[5] Young S L, Chen Y C, Horng L, Wu T C, Chen H Z and Shi J B 2000 *J. Magn. Magn. Mater.* **289** 145
[6] Blasse G 1965 *J. Phys. Chem. Solids* **26** 1969
[7] Goodenough J B, Wold A, Arnott R J and Menyuk N 1961 *Phys. Rev.* **124** 373
[8] Jonker J-H 1966 *J. Appl. Phys.* **37** 1424
[9] Park J-H, Cheong S-W and Chen C T 1997 *Phys. Rev.* B **55** 11072
[10] Toulemonde O, Studer F, Barnabe A, Maignan A, Martin C and Raveau B 1998 *Eur. Phys. J.* **4** 159
[11] Nishimori N, Asai K and Mizoguchi M 1995 *J. Phys. Soc. Japan* **64** 1326
[12] Toulemonde O, Studer F and Raveau B 2001 *Solid State Commun.* **118** 107
[13] Barilo S N, Bychkov G L, Kurnevich L A, Shiryaev S V, Kurochkin L A, Lynn J W and Vasiliu-Doloc L 2000 *J. Cryst. Growth* **211** 480
[14] Jeżowski A, Mucha J and Pompe G 1987 *J. Phys. D: Appl. Phys.* **20** 1500
[15] Mukovskii Ya M, Bebenin N G, Shulyatev D A and Arkhipov V E 2000 *Program and Abstract of the 18th General Conf. of the Condensed Matter Division (CMD-18) (Montreux, Switzerland, March 2000)* p 207
[16] von Helmolt R, Wecker J, Holzapfel B, Shhultz L and Samwer K 1993 *Phys. Rev. Lett.* **71** 2331
[17] Berman R 1976 *Thermal Conduction in Solids* (Oxford: Clarendon)
[18] Cohn J L, Popoviciu C P, McClellan K J and Leventouri Th 1997 *Phys. Rev.* B **56** R8495
[19] Visser D W, Ramirez A P and Subramianian M A 1997 *Phys. Rev. Lett.* **78** 3947

[20] Salamon M B and Jaime M 2001 *Rev. Mod. Phys.* **73**
[21] Troyanchuk I O, Bushynski M V, Szymczak H, Bärner K and Maignan A 2002 *Eur. Phys. J.* **28** 75
[22] Ju H L, Sohn H-C and Krishnan K M 1997 *Phys. Rev. Lett.* **79** 3230
[23] Park J-H, Vescovo E, Kim H-J, Kwon C, Ramesh R and Venkatesan T 1998 *Nature* **392** 794
[24] Jaime M, Lin P, Salamon M B and Han P D 1998 *Phys. Rev.* B **58** R5901
[25] Barnard R D 1972 *Thermoelectricity in Metals and Alloys* (London: Taylor and Francis) p 217
[26] Mandal P 2000 *Phys. Rev.* B **61** 14675
[27] Wasscher J D and Haas C 1964 *Phys. Lett.* **8** 302